

Synthesis, characterization and *in-vitro* cytotoxic potential of sitagliptin phosphate nanoparticles against advanced breast cancer cell line - MCF-7

Muhammad Abdullah¹, Azra Rafiq^{2,7}, Nariman Shahid², Muhammad Nasir Kalam⁴, Yusra Munir⁵, Muhammad Daoud Butt⁶ and Hamid Saeed²

¹Department of Pharmacy, Punjab University College of Pharmacy, University of the Punjab, Lahore, Pakistan

²Department of Pharmacy, University of Lahore, Lahore, Pakistan

³Middle East Technical University, Ankara, Turkey

⁴Department of Pharmacy, The Sahara University, Narowal, Pakistan

⁵Department of Pharmacy, Bahauddin Zakariya University, Multan, Pakistan

⁶School of Pharmaceutical Sciences, Universiti Sains Malaysia, Malaysia

⁷Department of Pharmacy, Riphah International University, Lahore, Pakistan

Abstract: Pharmaceutical substance sitagliptin has long been used to treat diabetes. However, subsequent researches have shown that sitagliptin has additional therapeutic effects. Anti-inflammatory effects are observed. Combining sitagliptin with biodegradable polymers like nanoparticles for chemotherapy may be effective. This method enhances therapeutic agent pharmacokinetics. This study tests sitagliptin (SIT) chitosan base nanoparticles against MCF-7 cancer cell lines for anti-cancer effects. Sitagliptin chitosan-based nanoparticles are tested for their ability to suppress MCF-7 cancer cell proliferation. Ionic gelation, a typical nanoparticle manufacturing method, was used. A detailed examination of the nanoparticles followed, using particle-size measurement, FTIR, and SEM. Entrapment efficiency, drug-loading, and *in-vitro* drug release were assessed. Loaded with chitosan and sitagliptin, the nanoparticles averaged 500nm and 534nm in diameter. Sitagliptin has little effect on particle size. Chitosan-based Sitagliptin nanoparticles grew slightly, suggesting Sitagliptin is present. SIT-SC-NPs had 32% encapsulation efficiency and 30% drug content due to their high polymer-to-drug ratio. SEM analysis showed that both drug-free and sitagliptin-loaded nanoparticles are spherical, as shown by the different bands in the photos. The SIT-CS-NPs had a 120-hour release efficiency of up to 80%. This suggests that these nanoparticles could cure hepatocellular carcinoma, specifically MCF-7 cell lines.

Keywords: Sitagliptin, chitosan nanoparticles, advanced breast cancer, *in-vitro* cytotoxicity, MCF-7 cell lines, nanoparticle-based chemotherapy.

INTRODUCTION

Cancer is a multifaceted collection of disorders that manifests as the unregulated proliferation and dissemination of abnormal cells, with the potential to arise in diverse bodily organs and tissues. Metastasis is a critical factor in cancer-related mortality, including the infiltration of adjacent tissues by cancer cells and their subsequent migration to distant organs. In the past decade, cancer was responsible for an estimated 9.6 million fatalities, thereby positioning it as the second most significant contributor to worldwide mortality (Ruddon, 2007; Warwick-Booth & Cross, 2018). The incidence rates of several types of cancer exhibit gender disparities, as seen by the predominance of lung, prostate, colorectal, stomach, and breast cancer among males and breast, colorectal, lung, cervical and thyroid cancer among females (Idrees *et al.*, 2018).

Cancer presents itself in several manifestations, encompassing carcinoma, melanoma, sarcoma, lymphoma and leukemia. Carcinomas, which originate from various

tissues such as the skin, lungs, breasts, pancreas and glands, represent the most commonly detected forms of cancer. (Demir, 2007 and Shaefer Jr *et al.*, 2015) Lymphomas are characterized by the impact on lymphocytes, while leukemia is characterized by the abnormal growth of blood cells (Stickel *et al.*, 2017). Sarcomas, on the other hand, develop from different types of connective tissues, while melanomas arise from skin cells responsible for pigment production (Ananthakrishnan *et al.*, 2006).

This study article explores a specific domain of oncology research, namely breast cancer, which is a widely prevalent disease that has a substantial impact on the health of women. Advanced breast cancer, namely the highly aggressive MCF-7 cell line, presents significant obstacles as a result of its propensity for aggressive activity and metastatic spread (Pei *et al.*, 2023).

In the setting of advanced breast cancer, the implementation of novel therapeutic approaches is important to combat its highly aggressive characteristics effectively. The repurposing of pre-existing

*Corresponding author: muhammaddaoud10@yahoo.com

pharmaceuticals and the utilization of sophisticated drug delivery technologies offer encouraging strategies for improving treatment efficacy (Losh, 2009). The primary objective of this study is to explore the potential of Sitagliptin Phosphate Nanoparticles as an innovative therapeutic approach for advanced breast cancer, with a specific emphasis on targeting the MCF-7 cell line (Kheraldine *et al.*, 2021).

This study presents a potential pathway for enhancing the outcomes of patients with advanced breast cancer by integrating the domains of nanotechnology and cancer research. This collaboration contributes to the continuous endeavors in addressing the challenges posed by this difficult disease (Nabil *et al.*, 2021). Considering the considerable incidence and consequential ramifications of breast cancer, particularly in advanced stages, the implementation of a novel and efficacious strategy has the potential to profoundly reshape therapy frameworks and enhance patient prognoses (Koundouros & Poulogiannis, 2020). The utilization of drug repurposing strategies, such as sitagliptin, which has demonstrated cytotoxic properties against cancer cells, presents a viable and economically efficient approach to improve treatment efficacy (Kirtonia *et al.*, 2021 and Lesmana *et al.*, 2006).

Cancer, an intricate assortment of diseases distinguished by unregulated cellular proliferation, represents a significant worldwide health issue owing to its profound influence on mortality rates (Tewari *et al.*, 2022). The metastatic phenomenon, characterized by the infiltration of cancer cells into adjacent tissues and subsequent migration to distant organs, plays a substantial role in cancer-related mortality (Bhat *et al.*, 2021). The differential occurrence rates of distinct cancer kinds among individuals of different genders highlights the necessity of implementing tailored strategies to effectively tackle the specific obstacles associated with each type (Kale *et al.*, 2023; Zapka & Lemon, 2004).

Breast cancer, a disease of significant prevalence and significance, poses a substantial challenge, particularly in its advanced stages. The necessity for alternative therapeutic techniques arises from the aggressive nature of advanced breast cancer, as demonstrated by the MCF-7 cell line. The utilization of pre-existing pharmaceuticals, such as Sitagliptin, has potential in augmenting the efficacy of treatment results (Malik *et al.*, 2022). In addition, the utilization of nanomedicine methodologies for the administration of therapeutic medicines via nanoparticles presents a promising advancement in the field of cancer treatment. The user has provided a reference to support their statement (Tiwari *et al.*, 2023).

The objective of this study is to produce and analyze sitagliptin phosphate nanoparticles and evaluate their cytotoxicity against MCF-7 cell lines in an *In-vitro* setting. This research endeavors to enhance the accessibility and effectiveness of treatment choices for

breast cancer patients in Pakistan and other regions by integrating drug repurposing with nanomedicine technology.

MATERIALS AND METHODS

The sitagliptin used in this study was obtained from Mass Pharmaceuticals Pvt. Limited, Lahore, with the batch number B#27-0001-21037 as gift sample. Glacial acetic acid (100%) was sourced from SIGMA-ALDRICH, identified by the RTECS number AF-1225000. Sodium tri-polyphosphate, with the lot number SBCC2990, was also acquired from SIGMA-ALDRICH. Chitosan, used in the study, was procured from SIGMA-ALDRICH and its lot number was STBH6262. The dialysis tubing used, with dimensions 14.3mm and a molecular weight cutoff (MWCO) of 12,000-14,000 Daltons, was obtained from Medicell Membranes Ltd.

The cell culture medium used for the study was Dulbecco's modified eagle medium (DMEM) with the product code L0102-500, sourced from Biowest, USA. Fetal bovine serum (FBS) was also used, obtained from Hyclone with the product code SV30160, originating from South America. The penicillin-streptomycin solution used was from Hyclone with the product code SV30082.01, sourced from the US. Phosphate-buffered saline (PBS) was procured from Oxoid, England, with the product code BR0014G. Thiazolyl tetrazolium bromide (MTT), a commonly used reagent, was sourced from Bioworld, USA, with the product code 42000092-2.

For experimental assays, 96-well plates were used, which were obtained from Corning, USA. The Breast cancer (MCF-7) cell lines utilized in the study were generously provided by the School of Biological Sciences (SBS) and the Center of Excellence in Molecular Biology (CEMB), Lahore, Pakistan.

Preparation of sitagliptin NPs

Sitagliptin nanoparticles (SIT-CS-NPs) were formulated using the ionic gelation method (Wilson, Alobaid, Geetha, & Jenita, 2021). The process involved dissolving chitosan in glacial acetic acid (2% v/v) and allowing it to stand overnight. SIT was dissolved in the prepared chitosan solution. The SIT-CS-NPs were created by adding tripolyphosphate (0.2% w/v) at a rate of 1 ml/min while continuously stirring at 600 RPM for 2 hours at room temperature. The resulting solution was poured into vials and centrifuged at 10,000 rpm for 30 minutes to obtain nanoparticles, which were then washed with double distilled water (Mittal *et al.*, 2022). Different batches with varying concentrations were prepared.

Drug encapsulation efficiency

The drug encapsulation efficiency (EE) was determined by assessing the amount of untrapped drug in the supernatant collected during the preparation of SIT-CS-

NPs. The concentration of untrapped drug was measured at the λ -max of SIT (256 nm) using a UV-absorbance spectrometer, and the encapsulation efficiency was calculated using the equation 1.

$$\text{Encapsulation Efficiency (EE)} = \frac{\text{Weight of drug in NPs}}{\text{Weight of initial drug}} \times 100\%$$

Drug loading

The drug loading (DL) of SIT in the prepared chitosan nanoparticles was quantified by comparing it with a standard solution of SIT using a UV-spectrophotometer. Absorbance was measured at the λ -max of SIT (256 nm), and the drug loading was calculated using the equation 2.

$$\text{Drug Loading (DL)} = \frac{\text{Weight of drug in NPs}}{\text{Weight of NPs}} \times 100\%$$

Characterization

Fourier Transform Infrared Spectroscopy (FTIR)

The FTIR spectra of chitosan polymer, chitosan nanoparticles, sitagliptin and SIT nanoparticles were obtained using the Agilent Cary 630 FTIR Spectrometer. Samples were prepared in KBr disks and scanned in the IR region of 4000-400 cm^{-1} .

Analysis of particle size

The particle size analysis of sitagliptin (SIT) nanoparticles and chitosan nanoparticles was conducted using the BT-90 Nano laser particle size analyzer. Nanoparticles were sonicated in deionized water to reduce particle adhesion, and the particle size was measured under specific conditions.

Scanning electron microscope-energy dispersive X-ray spectroscopy (SEM-EDX)

The Nova NanoSEM 450 field-emission scanning electron microscope (FE-SEM) was utilized to study the surface morphology of SIT-Chitosan NPs and chitosan nanoparticles. Prior to imaging, the samples underwent a gold coating process in a vacuum environment.

In-vitro drug release study

The *In-vitro* drug release of sitagliptin from chitosan nanoparticles was assessed using the dialysis method. Samples of SIT nanoparticles were placed in dialysis tubing and subjected to a dissolution medium. The concentration of released SIT was measured using a UV spectrophotometer and the cumulative release over time was determined.

Cytotoxic assay

The cytotoxic effects of free and encapsulated sitagliptin nanoparticles against MCF-7 cell lines were assessed using the MTT assay (Ghasemi, Turnbull, Sebastian & Kempson, 2021). MCF-7 cells were treated with varying concentrations of SIT nanoparticles and cell viability was measured through absorbance readings.

STATISTICAL ANALYSIS

The experimentation protocol was replicated thrice and the resultant data were presented as mean \pm standard

deviation (SD). Statistical analyses were executed using GraphPad Prism software (version 7). Subsequently, the data underwent rigorous statistical scrutiny employing both analysis of variance (ANOVA) and Tukey's post hoc test, facilitated by GraphPad Prism, version 7. Significance was ascribed to findings with a p-value less than 0.05.

RESULTS

In this present study, SIT-CS-NPs were prepared by using the effective biodegradable polymer named chitosan. The SIT-CS-NPs were prepared by using the ionic gelation method and then characterized by the various techniques for the determination of the physiochemical properties. The cytotoxic assay of these nanoparticles is performed to be investigation against the anti-cancer properties of these nanoparticles for breast carcinoma cells.

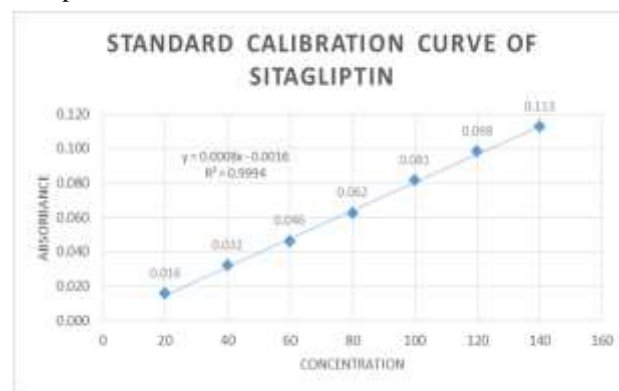


Fig. 1: Calibration curve of sitagliptin

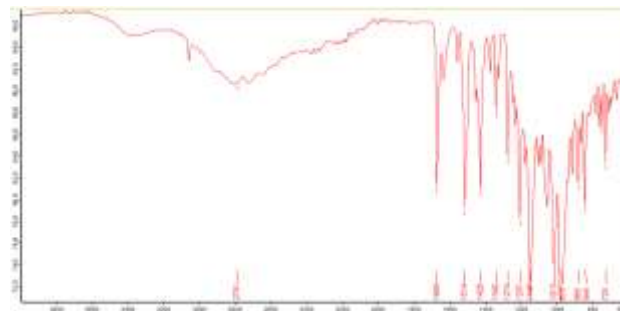


Fig. 2: FTIR of sitagliptin raw

Percentage entrapment efficacy

The percentage-entrapment-efficiency of the prepared nanoparticles was determined by using equation 1. Percentage Entrapment efficiency of SIT-CS-NPs has been measured after taking the mean of 3 preparations.

Drug loading capacity

The drug loading capacity of prepared SIT nanoparticles was determined by using Equation 2. The calibration curve was measured for Sitagliptin to determine the concentration of unknown samples as it was illustrated in the fig. mentioned below.

Table 1: Sitagliptin NPs various concentration

Ingredients	Batch 1	Batch 2	Batch 3
Sitagliptin (mg)	50	100	250
Chitosan (mg)	50	100	250
Glacial Acetic Acid (ml, 2% v/v)	30	30	30
Tripolyphosphate (ml, 0.2% w/v)	15	15	15

Table 2: Percentage entrapment efficacy

Formulation	Particle size(nm)	PDI	EE (%)	LC (%)
NP's Empty	500nm	0.076	-	-
NP's + SIT	526nm	0.069	32%	30%

Table 3: In-vitro drug release

% Drug Release				
	mg	mL	mg/mL	Abs of STD
STD	0.5	50	0.01	0.04
SMP	33.8	30	1.1267	
Sitagliptin Nanoparticles				
Time (hrs)	Abs of SMP	Cumulative Drug Release %	Correction Factor	
0	0	0	0	
0.25	0.125	2.774	0.277	
0.3	0.213	5.004	0.455	
1	0.356	8.354	0.696	
2	0.452	10.726	0.825	
4	0.632	14.849	1.086	
6	0.963	22.455	1.497	
8	1.563	36.179	2.261	
12	2.456	56.758	3.339	
24	3.135	72.902	4.050	
48	3.622	84.420	4.443	
72	3.865	90.205	4.510	

Table 4: Percentage drug release by NPs

% Drug Release			
	mg	mL	mg/mL
STD	0.5	50	0.01
SMP	35	30	1.1667
Sitagliptin Raw drug			
Time (hrs)	Abs of SMP	Cumulative Drug Release %	Correction Factor
0	0	0	0
0.25	2.236	47.914	4.791
0.3	3.232	74.049	6.732
1	3.589	83.639	6.970
2	3.756	87.456	6.727
4	3.963	91.649	6.546
6	4.125	94.939	6.329
8	4.253	97.465	6.092
12	4.375	99.842	5.873

Fourier-transfer-infrared-analysis (FTIR)

The prepared SIT nanoparticles were subjected to the Fourier transfer infrared analysis (FITR) for the determination of characteristics of peaks of pure drug in final prepared nanoparticles with polymer (chitosan). The spectrum of pure Sitagliptin, polymer and final formulation were recorded and compared with each other.

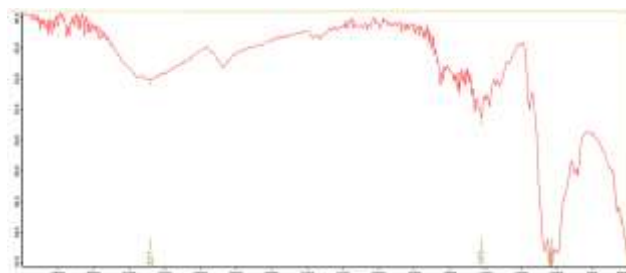


Fig. 3: Chitosan raw FTIR

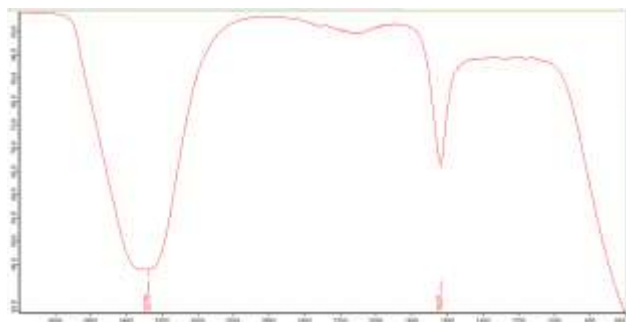


Fig. 4: FTIR of sitagliptin chitosan Base NPs

FTIR analysis of sitagliptin phosphate nanoparticles

A total of four sets of Fourier Transform Infrared (FTIR) spectra were acquired, encompassing the analysis of pure sitagliptin or sitagliptin raw, chitosan, sitagliptin Nanoparticles (NPs) and the resultant formulations. The Fourier-transform infrared (FT-IR) spectrum of sitagliptin phosphate and sitagliptin nanoparticles displays several distinctive bands. A prominent characteristic is the presence of a robust broad-band at 3357cm^{-1} , which can be ascribed to the stretching vibration of the N-H bond. In contrast, the stretching vibration shown by the NH_2 group is quite feeble. Furthermore, there were medium strong-bands detected at wave numbers of 3059cm^{-1} , 2917cm^{-1} and 2850cm^{-1} , which can be attributed to the stretching vibrations of C-H bonds present in both aromatic and aliphatic functional groups. Within the spectral region spanning from 1669cm^{-1} to 1634cm^{-1} , one can observe the presence of medium-to-be-strong bands. These bands can be ascribed to the vibration-stretching of both the carbonyl group and the 1,2,4-triazole ring. The peak that is prominently detected at a wavenumber of 1609cm^{-1} is most likely attributed to the vibrational motion of N-H bending. The stretching vibrations of -C-N and -C-N bonds can be ascribed to the three bands detected at the wavenumbers 1556 , 1514 and 1426cm^{-1} . The vibrational frequencies detected at 1324 and 1274cm^{-1} were indicative of the in-plane bending motion exhibited by the

C-H bonds. In contrast, the spectral bands observed at 1146 and 978cm^{-1} were indicative of the stretching vibration associated with the C-F bonds. The spectral patterns seen at wavenumbers 913 , 881 , 844 and 725cm^{-1} display discernible characteristics that suggest the presence of out-of-plane bending.

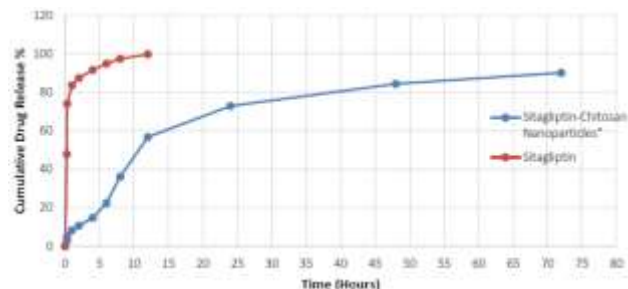


Fig. 5: *In-vitro* drug release sitagliptin-loaded chitosan nanoparticles

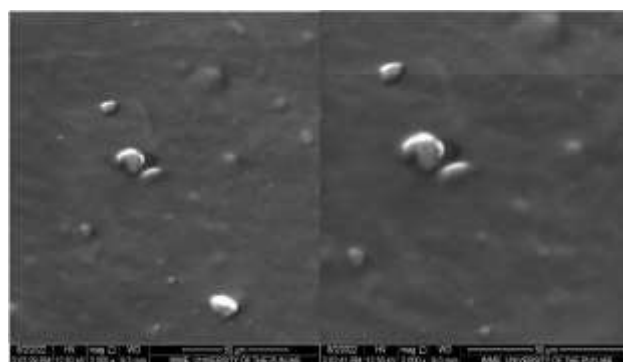


Fig. 6: SEM Image of SIT-NPs (50 to 100 micrometer)

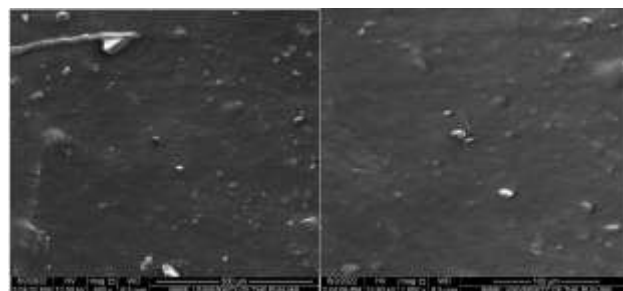


Fig. 7: SEM images of SIT-NPs (100-300 micrometer)

The chelation process results in a noticeable decrease in the frequency values of the stretching vibration of the -NH_2 base group, which were seen at 3300 , 3316 , 3340 , 3341 , 3305 and 3340cm^{-1} . The Fourier-transform infrared (FT-IR) spectra of the chitosan nanoparticles (NPs) demonstrate the lack of bands that were typically linked to the bending vibration of the -NH_2 functional group. This observation implies that the chelation mechanism between the ST ligand and chitosan.

involves the bonding of the ST ligand to a nitrogen atom inside the NH_2 group. The wavenumber at which the vibrational stretching of the (C=O) groups in the unbound ST ligand occurs is measured to be 1669cm^{-1} .

Nevertheless, the observed peak is absent in the spectra of ST NPs, as is the case with several other nanoparticles. This observation implies that the oxygen atom and C=O group could participate in chelation with other pharmaceutical compounds.

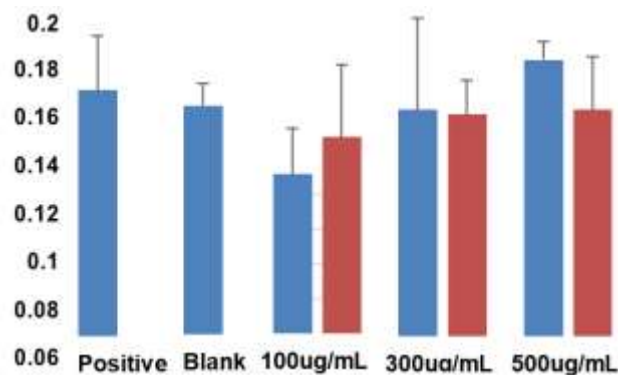


Fig. 8: MTT assay results cell viability of MCF-7 cells sitagliptinr vs sitagliptin NPs, blue SIT raw, red is SIT-NPs.

The observed spectral bands at a wavenumber of 1634 cm^{-1} in the synthesized silver nanoparticles (ST-NPs) were attributed to the stretching-vibration of the carbon-nitrogen (C=N) bond inside the 1,2,4-triazole ring. The bands observed in the ST NPs demonstrate minimal or slightly elevated wave numbers, suggesting that the nitrogen atom inside the C=N group does not actively participate in the coordination process. The chemical known as Free ST demonstrates two different stretching bands, which were observed at wave numbers of 1146 and 978 cm^{-1} , specifically inside the -C-F area. After the formation of NP structures, it is noted that the maxima stay constant, suggesting that the C-F bond is quite distant from the location of complexity. The presence of spectral peaks with moderate to low intensity in the frequency range of 558-445 cm^{-1} suggests the participation of Chitosan in stretching vibrations of oxygen and nitrogen atoms. Hence, the findings from the infrared spectroscopy analysis indicate that chitosan establishes coordination bonds with the ST phosphate. The ligand demonstrates bidentate chelation characteristics, as illustrated in the pictures, by utilizing its amino and carbonyl functional groups.

Analysis of particle size

The particle size of chitosan-based nanoparticles of Sitagliptin (SIT) were determined using particle size analyzer-BT-90

Particle size of SIT NPs

The results of the particle size study indicate that the particles of chitosan NPs were uniformly dispersed, with an average size of 500nm and a polydispersity index of 0.076 ± 0.054 . Regarding SIT-NPs, it was observed that they exhibited an average diameter measuring 534nm, accompanied by a polydispersity index of 0.084.

In-vitro drug release

The dialysis method is used to determine the *in-vitro* release of chitosan-based Sitagliptin phosphate nanoparticles at a pH of 7.4. Results were shown mentioned below in the fig. 5. This formulation shows the biphasic releasing pattern with an initial burst or abrupt release of the drug followed early few hours and two hours and sustained release of chitosan NPs through 3 days.

SEM analysis of sitagliptin chitosan nanoparticles

Scanning electron microscopy (SEM) is carried out to determine the morphology of the chitosan-based sitagliptin nanoparticles. When observed using SEM, mentioned below fig. shows this polymer nanoparticles have a smooth-globular-surface with some kind of variations, mostly due to having a sucrose-solution embedded which is being used as a cryoprotectant when-freeze-drying

Cytotoxic assay

This study included cytotoxic effects of free sitagliptin and the different concentrations of the SIT-CS-NPs NPs on the MCF-7 cancer cells after 24 hours of incubation and then being assessed using a colorimetric MTT assay. MTT assay - results of the cytotoxic activity against the MCF-7 cells were shown in the below fig. This indicates that SIT-CS-NPs have very comparable or no significant difference of cytotoxic effect in raw and NPs forms of sitagliptin.

DISCUSSION

It is widely recognized that the glucose-lowering benefits of sitagliptin were currently being investigated for potential off-label applications. The incretin actions of DDP4 have been observed to contribute to cardiac safety and the regulation of hypertension (Lytvyn *et al.*, 2017). Consequently, there is potential for future investigation into the potential of this medicine in cancer prevention and its anti-cancer activities. Upon careful examination of the patient's medical history, profile and the severity of the condition, it is evident that Sitagliptin demonstrates significant efficacy and favourable benefits in the treatment of diverse metabolic diseases, certain neurogenerative disorders, as well as renal and bone disorders (Islam *et al.*, 2022). There has been an increased interest in exploring the potential applications of sitagliptin as an agent or medicine for treating liver cancer and breast cancer, either as a standalone treatment or in conjunction with other chemotherapeutic agents. Previous epidemiological research demonstrated that the consumption of sitagliptin significantly enhances clinical outcomes in different types of cancer (Garg *et al.*, 2014). However, the limited bioavailability, short half-life and adverse effects of Sitagliptin pose obstacles to its potential application as a chemotherapeutic agent. Sitagliptin phosphate is classified under the

Biopharmaceutics Classification System (BCS) as Class 3, indicating that it is a highly soluble medication with limited permeability. One potential technique for enhancing the availability of a substance is by the conversion of its nanoparticles, which can help overcome its poor permeability and modify its physiological feature (Talegaonkar & Bhattacharyya, 2019). The findings of this work demonstrate that chitosan-loaded sitagliptin nanoparticles exhibit significant cytotoxic effects on MCF-7 cells, surpassing the cytotoxicity observed with normal sitagliptin or raw sitagliptin.

In recent years, the use of non-biodegradable polymers in pharmaceutical sciences has raised concerns, leading to the exploration of biodegradable polymers as an alternative solution. Due to growing concerns over environmental safety and the escalating issue of global warming, consumers have noticed a notable rise in the use of biopolymers. Biopolymers exhibit less adverse environmental impacts and can be readily obtained from various sources such as agricultural raw materials, marine organisms, microorganisms and wildlife. The waste generated by these companies can potentially be exploited for the manufacturing of biopolymers. Chitosan has garnered significant interest in nanostructure formulation due to its complete biodegradability, biocompatibility, tunable physiochemical characteristics, ease of processing and well-defined formulation processes (Al Sharabati *et al.*, 2021). Chitosan has been utilised not only as a carrier in various drug delivery methods but also as a framework in tissue engineering. Chitosan has significantly benefited from facilitating complete biodegradation in aquatic environments (Wankar *et al.*, 2020). The product has received approval from the Food and Drug Administration (FDA). It has garnered considerable attention due to its notable efficacy features, such as biocompatibility, versatility in designing sustained-release formulations, protection of drugs or agents from degradation and potential targeting of specific organ cells. Compelling arguments for using chitosan as the preferred material for creating desired medication nanoparticles have been previously discussed (Upadhyaya *et al.*, 2014).

Primary human breast cancer cell lines were widely regarded as the gold standard for *in-vitro* investigations about liver-specific toxicity and xenobiotic metabolism (Guillouzo *et al.*, 2007). However, their utilisation is hindered by limited availability resulting from a scarcity of human breast cell samples and their short lifespan and high costs. An alternate methodology to primary human breast cancer cell involves the utilization of two-dimensional (2D) monolayers (Gómez-Lechón *et al.*, 2014). The MCF-7 Breast cancer cell line was initially derived from breast cancer in a thirty-year-old female subject of Caucasian-American descent. MCF-7 cells were a widely recognized breast cancer cell line that serves as an established and commonly utilized *In-vitro* model for human breast cancer cells. During the process

of cultivation, MCF-7 cells secrete many liver-specific plasma proteins, such as transferrin, α -fetoprotein, and albumin. The user's text is a numerical value. The MCF-7 cells are not only extensively utilized as a model for human breast cells, but they are also considered to be straightforward and manageable under *in-vitro* settings, allowing for the generation of reliable and accurate data over an extended period of time (Ramirez *et al.*, 2018). The observed characteristics of these entities include non-tumorigenic behavior, a significantly elevated growth rate, an epithelial-like appearance, and the ability to execute numerous distinct breast functions. MCF-7 cells have been successfully cultured on a bigger scale in a culture system. The examination of MCF-7 cells reveals the expression of differentiated breast functions, including lipoprotein metabolism and transport, synthesis and secretion of plasma proteins, cholesterol and triglyceride metabolism, glycogen synthesis, insulin signaling, and bile acid synthesis (Kouhbanani *et al.*, 2021; Maurya, 2009; Van Landeghem). Therefore, the MCF-7 cell lines were selected for our investigation of breast cancer (Aslan *et al.*, 2004).

Spherical inorganic-organic hybrid nanoparticles (SIT-CS-NPs) are synthesized using the ionic gelation technique, which is subsequently followed by freeze-drying (Faramarzi *et al.*, 2019). Numerous studies in literature have employed the same methodology for synthesizing Chitosan sitagliptin nanoparticles (SreeHarsha *et al.*, 2019; Thondawada *et al.*, 2018). The present study aimed to characterize Sitagliptin chitosan nanoparticles in order to investigate their physiochemical characteristics and shape. The SIT-CS nanoparticles exhibited an entrapment efficiency (EE) of 33%, as indicated (Amritha *et al.*, 2015). The drug content (DC) was also reported. This indicates that the encapsulation of sitagliptin was highly successful, as observed through the chosen methodology and at larger concentrations of sitagliptin, the values for DC and EE began to decrease. The particle-size measurements of the sitagliptin nanoparticles, as indicated in the table, provide suggestive evidence. There are numerous aspects to consider, such as the viscosity of the media. The factors to consider in polymer concentration, drug-polymer ratio, type and concentration of stabilizing agents, and the organic-phase/aqueous-phase ratio, as well as the kind of organic solvents, are important in this context. The particle size of polymeric drug delivery systems is influenced by various factors (Gundogdu & Cetin, 2014; Guo *et al.*, 2020). As a result, the particle size of these chitosan sitagliptin nanoparticles was influenced by the high drug-to-polymer ratio. The polydispersity index is a metric that quantifies the degree of heterogeneity in the molecular weight distribution of a polymer's polymeric chain. It has been shown that nanoparticles generated in this study exhibit a polydispersity index (PDI) value of less than 0.1, indicating a limited distribution of polymer and a monodisperse system.

A scanning electron microscopy (SEM) analysis was conducted in order to investigate the morphology and composition of the synthesized polymeric nanoparticles. The scanning electron microscopy (SEM) analysis of nanoparticles based on Chitosan revealed a clean circular surface with minimal aggregation. One potential explanation for the phenomenon of agglomeration could be attributed to the accumulation process that takes place during ion-sputtering involving gold.

The Dialysis method was employed to investigate the release of sitagliptin from a chitosan polymer under pH 7.4 conditions. The results of this investigation are presented, which displays the observed releasing pattern. The initial three-hour period is characterized by the observation of a burst release, which is subsequently followed by a steady release over the next 72 hours. During this sustained release phase, approximately 82% of sitagliptin is released. According to the drug release analysis, the phenomenon of first burst release can be attributed to the presence of absorbed or encapsulated SIT (active ingredient) in close proximity to the surfaces of the nanoparticles (NPs). This proximity leads to a significantly greater breakdown rate of the Chitosan (polymer matrix) near the surface, resulting in an enhanced release of SIT (El-Naggar *et al.*, 2023).

However, the disparity between the medicine in its raw form and the drug encapsulated in a delivery system is not substantial. The percentage survivability of the two forms exhibits only a minimal variance. To date, research has been undertaken on the nanoencapsulation of SIT with the aim of its potential application in the treatment of type 2 diabetes (Rofeal *et al.*, 2022). Nevertheless, the application of chitosan-based nanoparticles (NPs) for the efficient administration of SIT to different types of cancer cells has not been extensively investigated in previous studies.

CONCLUSION

In this study, chitosan base sitagliptin nanoparticles were effectively synthesized using the ionic gelation technique. Particle size and morphological analysis revealed that the SIT- SC-NPs exhibited spherical shapes with smooth surfaces with an average particle size <550nm. The formulated nanoparticles had desired or prescribed encapsulation efficiency and a sustained release profile revealing that they can be conveniently used for that purpose. Furthermore, the anticancer efficiency of chitosan base sitagliptin nanoparticles against MCF-7 cells showed a dose-related response. These findings indicate that the encapsulation of sitagliptin in the form of nanoparticles can offer an attractive drug delivery approach for the treatment of breast cancer. Further, in vivo examination ought to be conducted to make clear the therapeutic efficacy of these nanoparticles.

Study limitations

Our study has certain limitations concerning the use of MCF-7 cell lines as an *in-vitro* breast carcinoma study model. The 2D cell lines MCF-7 have the shortcomings of cross-contamination with other cell lines and susceptibility to genetic drift after long-term culturing. This leads to considerable deviation in in vivo response. Furthermore, because 2D cultured cells are constricted to adhere to a rigid surface, they adopt a flat morphology which affects normal cellular functions such as proliferation, signaling, migration, and apoptosis. Therefore, the use of three-dimensional (3D) models can be investigated to overcome the constraints.

REFERENCES

- Al Sharabati M, Abokwiek R, Al-Othman A, Tawalbeh M, Karaman C, Orooji Y and Karimi F (2021). Biodegradable polymers and their nano-composites for the removal of endocrine-disrupting chemicals (EDCs) from wastewater: A review. *Environ. Res.*, **202**: 111694.
- Amritha C, Kumaravelu P and Chellathai DD (2015). Evaluation of anti cancer effects of DPP-4 inhibitors in colon cancer-an invitro study. *JCDR*, **9**(12): FC14.
- Ananthakrishnan A, Gogineni V and Saeian K (2006). Epidemiology of primary and secondary liver cancers. Paper presented at the Seminars in interventional radiology. Copyright© 2006 by Thieme Medical Publishers, Inc., 333 Seventh Avenue, New York, NY 10001, USA. **23**(1): 047-063
- Aslan M, Afşar E, Kırımloğlu E, Çeker T and Yılmaz Ç (2021). Antiproliferative effects of thymoquinone in MCF-7 breast and HepG2 liver cancer cells: Possible role of ceramide and ER stress. *Nutr. Cancer*, **73**(3): 460-472.
- Bhat AA, Nisar S, Maacha S, Carneiro-Lobo TC, Akhtar S, Siveen KS and Singh M (2021). Cytokine-chemokine network driven metastasis in esophageal cancer; promising avenue for targeted therapy. *Mol Cancer.*, **20**(1): 1-20.
- Demir K (2007). Molecular Karyotyping of Human Hepatocellular Carcinoma Cell Lines Using Single-Nucleotide Polymorphism Arrays. Bilkent Universitesi (Turkey), PhD diss., Bilkent Universitesi (Turkey).
- El-Naggar ME, El-Rafie M, El-Sheikh MA, El-Feky GS, and Hebeish A (2015). Synthesis, characterization, release kinetics and toxicity profile of drug-loaded starch nanoparticles. *Int. J. Biol. Macromol.*, **81**(2015): 718-729.
- Faramarzi L, Dadashpour M, Sadeghzadeh H, Mahdavi M and Zarghami N (2019). Enhanced anti-proliferative and pro-apoptotic effects of metformin encapsulated PLGA-PEG nanoparticles on SKOV3 human ovarian carcinoma cells. *Artif Cells Nanomed Biotechnol*, **47**(1): 737-746.

- Garg S, Maurer H, Reed K and Selagamsetty R (2014). Diabetes and cancer: Two diseases with obesity as a common risk factor. *Diabetes Obes Metab*, **16**(2): 97-110.
- Ghasemi M, Turnbull T, Sebastian S and Kempson I (2021). The MTT assay: utility, limitations, pitfalls, and interpretation in bulk and single-cell analysis. *Int. J. Mol. Sci.*, **22**(23): 12827.
- Gómez-Lechón MJ, Tolosa L, Conde I and Donato MT (2014). Competency of different cell models to predict human hepatotoxic drugs. *Expert Opin Drug Metab Toxicol*, **10**(11): 1553-1568.
- Guillouzo A, Corlu A, Aninat C, Glaise D, Morel F and Guguen-Guillouzo C (2007). The human hepatoma HepaRG cells: A highly differentiated model for studies of liver metabolism and toxicity of xenobiotics. *Chem. Biol. Interact*, **168**(1): 66-73.
- Gundogdu N and Cetin M (2014). Chitosan-poly (lactide-co-glycolide)(CS-PLGA) nanoparticles containing metformin HCl: Preparation and *in vitro* evaluation. *Pak. J. Pharm. Sci.*, **27**(6): 1923.
- Guo W, Xu B, Wang X, Zheng B, Du J and Liu S (2020). The analysis of the anti-tumor mechanism of ursolic acid using connectively map approach in breast cancer cells line MCF-7. *Cancer Manag Res*, pp.3469-3476.
- Idrees R, Fatima S, Abdul-Ghafar J, Raheem A and Ahmad Z (2018). Cancer prevalence in Pakistan: meta-analysis of various published studies to determine variation in cancer figures resulting from marked population heterogeneity in different parts of the country. *World J Surg Onc*, **16**(1): 1-11.
- Islam S, Wang S, Bowden N, Martin J and Head R (2022). Repurposing existing therapeutics, its importance in oncology drug development: Kinases as a potential target. *Br. J. Clin. Pharmacol.*, **88**(1): 64-74.
- Kale S, Hirani S, Vardhan S, Mishra A, Ghode DB, Prasad R and Wanjari M (2023). Addressing cancer disparities through community engagement: Lessons and best practices. *Cureus*, **15**(8): e43445.
- Kheraldine H, Rachid O, Habib AM, Al Moustafa AE, Benter IF and Akhtar S (2021). Emerging innate biological properties of nano-drug delivery systems: A focus on PAMAM dendrimers and their clinical potential. *Adv. Drug Deliv. Rev.*, **178**: 113908.
- Kirtonia A, Gala K, Fernandes SG, Pandya G, Pandey AK, Sethi G and Garg M (2021). Repurposing of drugs: An attractive pharmacological strategy for cancer therapeutics. *Semin. Cancer Biol.*, **68**: 258-278.
- Kouhbanani MAJ, Sadeghipour Y, Sarani M, Sefidgar E, Ilkhani S, Amani AM and Beheshtkhoo N (2021). The inhibitory role of synthesized Nickel oxide nanoparticles against Hep-G2, MCF-7 and HT-29 cell lines: The inhibitory role of NiO NPs against Hep-G2, MCF-7 and HT-29 cell lines. *GCLR*, **14**(3): 444-454.
- Koundouros N and Poulogiannis G (2020). Reprogramming of fatty acid metabolism in cancer. *BJC*, **122**(1): 4-22.
- Lesmana LA, Leung NWY, Mahachai V, Phiet PH, Suh DJ, Yao G and Zhuang H (2006). Hepatitis B: overview of the burden of disease in the Asia-Pacific region. *Liver Int.*, **26**(S2): 3-10.
- Li Y, Cheng KC, Liu IM and Cheng JT (2023). Identification of andrographolide as an agonist of bile acid tgr5 receptor in a cell line to demonstrate the reduction in hyperglycemia in type-1 diabetic rats. *Pharmaceuticals*, **16**(10): 1417.
- Losh EM (2009). *Virtualpolitik: An electronic history of government media-making in a time of war, scandal, disaster, miscommunication, and mistakes*: MIT Press.
- Lytvyn Y, Bjornstad P, Udell JA, Lovshin JA and Cherney DZ (2017). Sodium glucose cotransporter-2 inhibition in heart failure: Potential mechanisms, clinical applications and summary of clinical trials. *Circulation*, **136**(17): 1643-1658.
- Malik JA, Ahmed S, Jan B, Bender O, Al Hagbani T, Alqarni A and Anwar S (2022). Drugs repurposed: An advanced step towards the treatment of breast cancer and associated challenges. *Biomed. Pharmacother*, **145**: 112375.
- Maurya P (2009). Identification of proteins associated with cancerous and invasive phenotypes of breast and melanoma cells using proteomic approaches. Dublin City University, PhD diss., Dublin City University, 2009.
- Mittal KR, Pharasi N, Sarna B, Singh M, Rachana Haider S and Dey A (2022). Nanotechnology-based drug delivery for the treatment of CNS disorders. *Transl. Neurosci.*, **13**(1): 527-546.
- Nabil G, Alzhrani R, Alsaab HO, Atef M, Sau S, Iyer AK and Banna HE (2021). CD44 targeted nanomaterials for treatment of triple-negative breast cancer. *Cancers*, **13**(4): 898.
- Pei S, Zhang P, Yang L, Kang Y, Chen H, Zhao S and Xie H (2023). Exploring the role of sphingolipid-related genes in clinical outcomes of breast cancer. *Front. Immunol*, **14**: 1116839.
- Ramirez T, Strigun A, Verlohner A, Huener HA, Peter E, Herold M and Spitzer M (2018). Prediction of liver toxicity and mode of action using metabolomics *in vitro* in HepG2 cells. *Arch. Toxicol.*, **92**: 893-906.
- Rofeal M, Abdelmalek F and Steinbuechel A (2022). Naturally-sourced antibacterial polymeric nanomaterials with special reference to modified polymer variants. *Int. J. Mol. Sci.*, **23**(8): 4101.
- Ruddon RW (2007). *Cancer biology*: Oxford University Press, pp.257-376.
- Shaefer Jr CF, Kushner P and Aguilar R (2015). User's guide to mechanism of action and clinical use of GLP-1 receptor agonists. *Postgrad. Med.*, **127**(8): 818-826.
- SreeHarsha N, Ramnarayanan C, Al-Dhubiab BE, Nair A B, Hiremath JG, Venugopala KN and Shariff A (2019).

- Mucoadhesive particles: A novel, prolonged-release nanocarrier of sitagliptin for the treatment of diabetics. *Biomed Res. Int.* 2019: Article ID 3950942
- Stickel F, Datz C, Hampe J and Bataller R (2017). Pathophysiology and management of alcoholic liver disease: Update 2016. *Gut Liver*, **11**(2): 173.
- Talegaonkar S and Bhattacharyya A (2019). Potential of lipid nanoparticles (SLNs and NLCs) in enhancing oral bioavailability of drugs with poor intestinal permeability. *AAPS PharmSciTech*, **20**: 1-15.
- Tewari D, Patni P, Bishayee A, Sah AN and Bishayee A (2022). Natural products targeting the PI3K-Akt-mTOR signaling pathway in cancer: A novel therapeutic strategy. Paper presented at the Seminars in Cancer Biology. **80**: 1-17.
- Thondawada M, Wadhvani AD, S Palanisamy D, Rathore HS, Gupta RC, Chintamaneni PK and Krishnamurthy PT (2018). An effective treatment approach of DPP-IV inhibitor encapsulated polymeric nanoparticles conjugated with anti-CD-4 mAb for type 1 diabetes. *Drug Dev. Ind. Pharm.*, **44**(7): 1120-1129.
- Tiwari H, Rai N, Singh S, Gupta P, Verma A, Singh AK and Gautam V (2023). Recent advances in nanomaterials-based targeted drug delivery for preclinical cancer diagnosis and therapeutics. *Bioengineering*, **10**(7): 760.
- Upadhyaya L, Singh J, Agarwal V and Tewari RP (2014). The implications of recent advances in carboxymethyl chitosan based targeted drug delivery and tissue engineering applications. *J Control Release*, **186**: 54-87.
- Van Landeghem J (2018). Cathepsin proteases in human breast cancer cell lines: Expression analysis and targeting by CRISPR/Cas9.
- Wankar J, Kotla NG, Gera S, Rasala S, Pandit A and Rochev YA (2020). Recent advances in host-guest self-assembled cyclodextrin carriers: Implications for responsive drug delivery and biomedical engineering. *Advanced Functional Materials*, **30**(44): 1909049.
- Warwick-Booth L and Cross R (2018). Global health studies: A social determinants perspective: John Wiley & Sons.
- Wilson B, Alobaid BNM, Geetha KM and Jenita JL (2021). Chitosan nanoparticles to enhance nasal absorption and brain targeting of sitagliptin to treat Alzheimer's disease. *J Drug Deliv Sci Technol*, **61**(1): 102176.
- Zapka JG and Lemon SC (2004). Interventions for patients, providers and health care organizations. *CA Cancer J. Clin.*, **101**(S5): 1165-1187.
- Zhang S (2004). Mechanisms of proliferation inhibition and apoptosis induced by vitamin E compounds and cyclooxygenase inhibitors in human breast cancer cells: The University of Texas at Austin. 202, p.694.